Supplement of

Evolution and drivers of urban–suburban ozone contrasts in China during 2013–2020

Ning Yang et al.

Correspondence to: Qiaoqiao Wang (qwang@jnu.edu.cn)

Table S1. Population densities (People per km^2) for different urban size categories (mean (min-max)) as well as suburban sites in Beijing, Tianjin, Ningbo, and Shenzhen.

Region	Suburban	Small cities (<0.5 million)	Medium cities (0.5-1 million)	Large cities (1-5 million)	Very large cities (5-10 million)	Mega cities (>10 million)	References
China	/	106 (39-264)	281 (18-667)	342 (6-1778)	564 (129-2501)	889 (409-2276)	/
Beijing	158-984	/	/	/	/	/	Li et al. (2022)
Tianjin	536	/	/	/	/	/	Han et al. (2013)
Ningbo	247-456	/	/	/	/	/	Tong et al. (2017)
Shenzhen	477-7607	/	/	/	/	/	Huang et al. (2018)

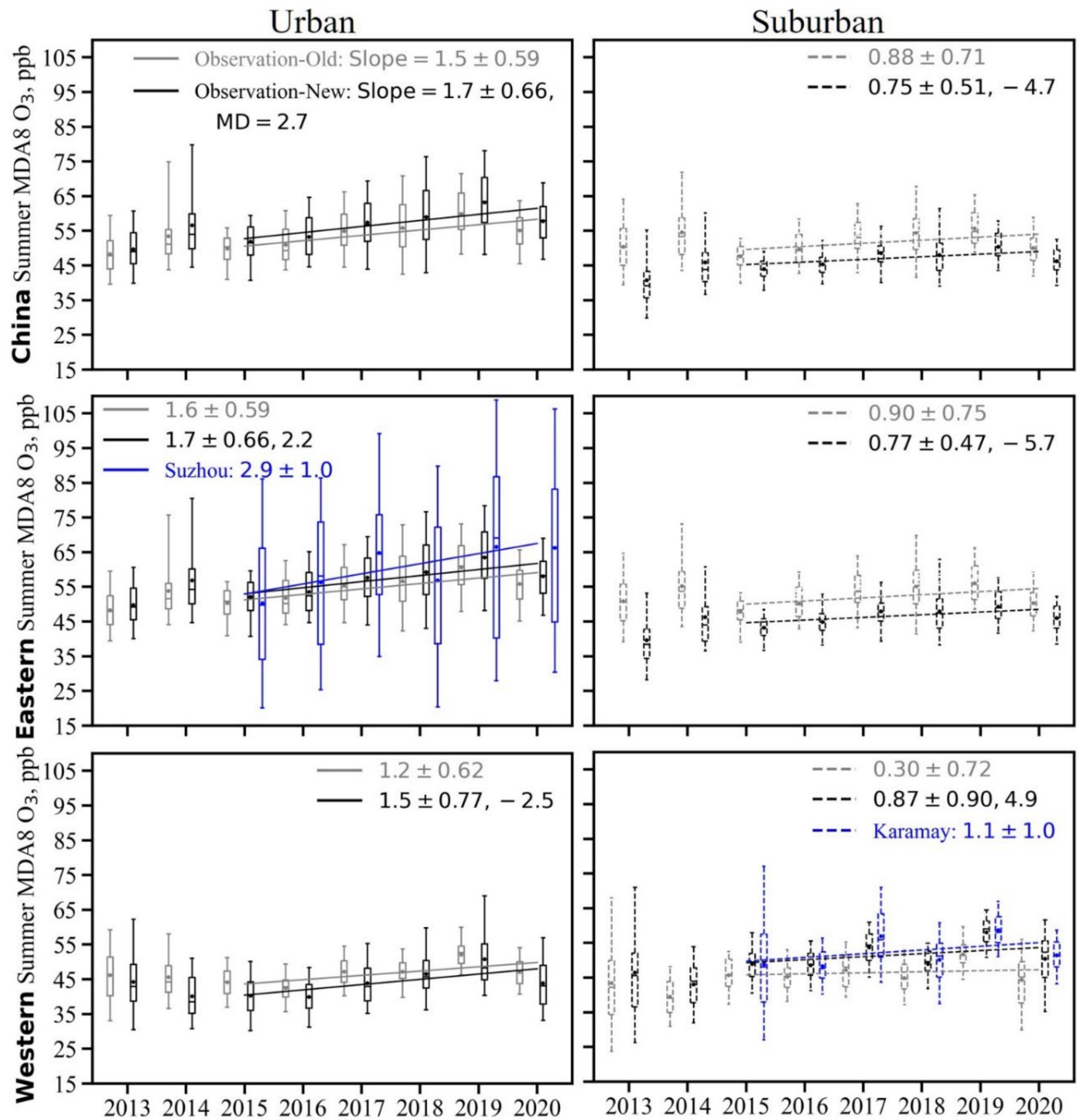

Figure S1. Observed summer O_3 trends at urban (left column) and suburban (right column) sites in China and subregions (Eastern and Western) from 2015 to 2020 based on the old (grey) and new (black) urban-suburban classifications, together with trends for two representative cities (Suzhou and Urumqi, blue). Fitted lines show linear trends, with slopes indicated and MD denotes the mean differences between the old and new classifications.

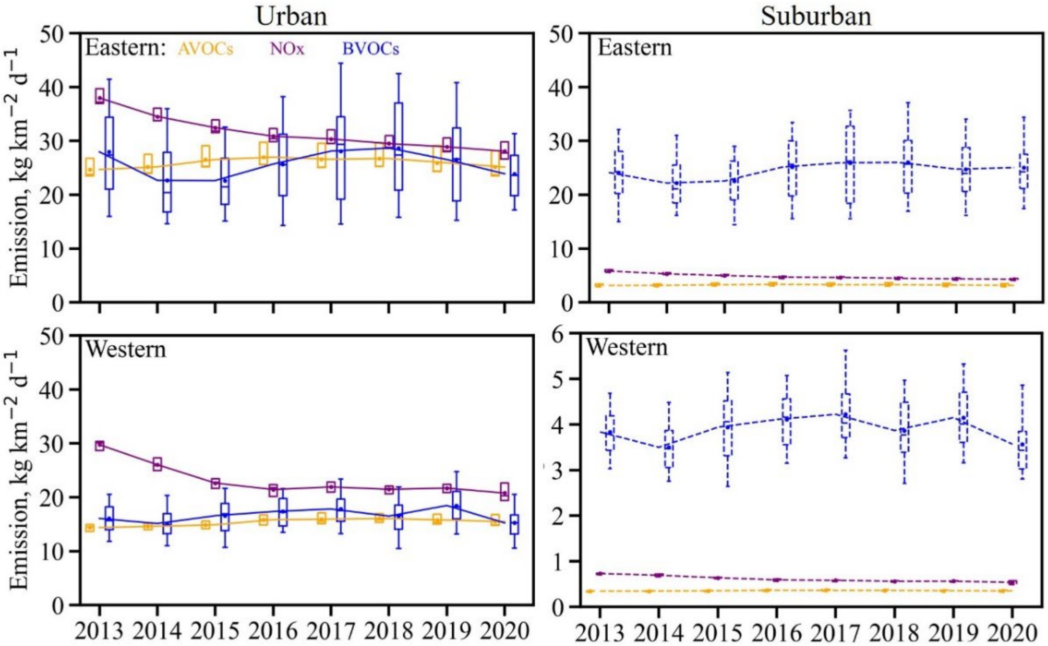

Figure S2. Temporal trends in summer AVOC, NOx, and BVOC emissions at urban (left column) and suburban (right column) sites across Eastern and Western China for the period 2013–2020.

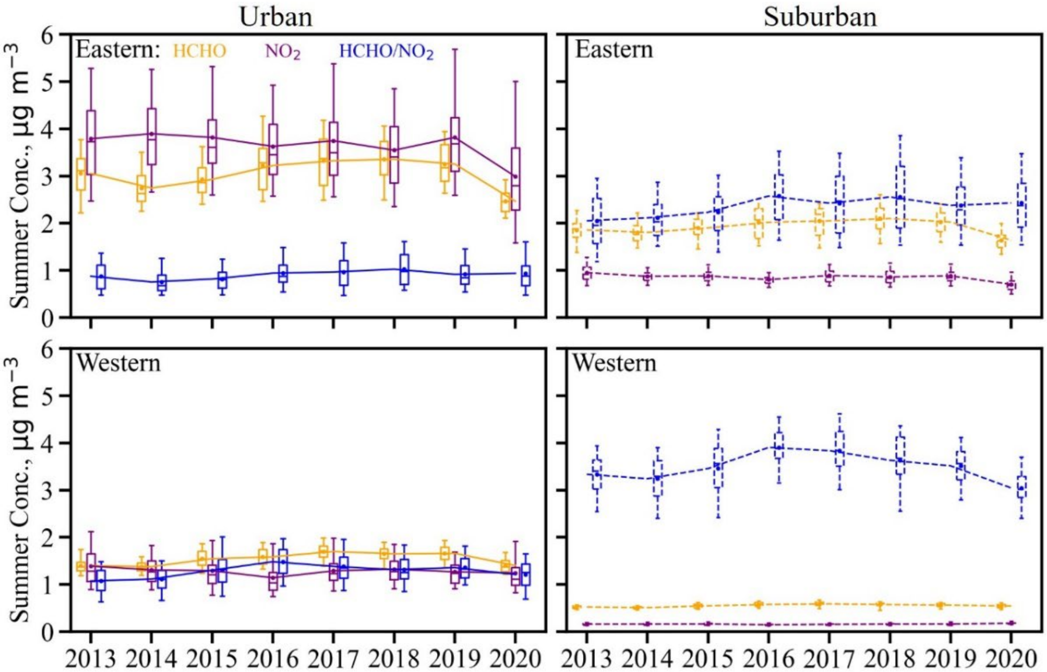

Figure S3. Temporal trends in summer HCHO, NO_2 concentrations and $HCHO/NO_2$ at urban (left column) and suburban (right column) sites across Eastern and Western China for the period 2013–2020.

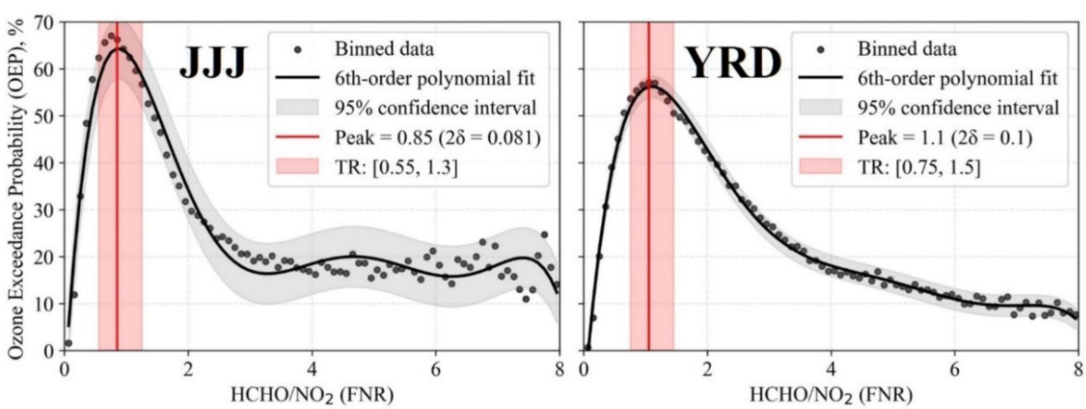

Figure S4. Probability of simulated O_3 exceeding 160 μg m^{-3} (ozone exceedance probability, OEP) as a function of simulated $HCHO/NO_2$ concentration ratio (FNR) for all sites in JJJ and YRD during summer from 2013 to 2020. The black curve represents the fitted six-order polynomial curves, and the shading indicates 95% confidence intervals. The vertical red line represents the peak value of the fitted value, and the vertical red shading is the range over the top 10% of the fitted curve (transition regime, TR).

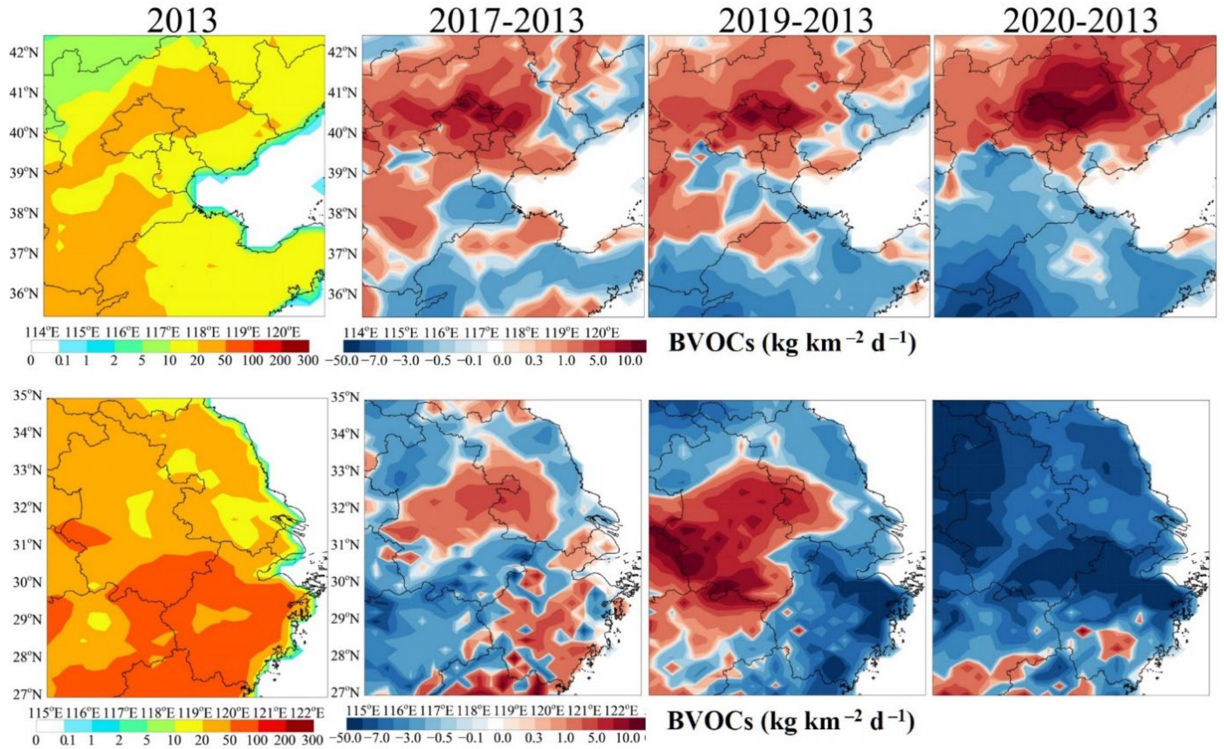

Figure S5. Spatial distribution of summer BVOCs emissions over the JJJ and YRD regions in 2013, together with the corresponding emission changes in 2017, 2019, and 2020 relative to 2013.

References:

Han, S.-q., Zhang, M., Zhao, C.-s., Lu, X.-q., Ran, L., Han, M., Li, P.-y., and Li, X.-j.: Differences in ozone photochemical characteristics between the megacity Tianjin and its rural surroundings, Atmos. Environ, 79, 209-216, https://doi.org/10.1016/j.atmosenv.2013.06.045, 2013.

Huang, D., Li, Q., Wang, X., Li, G., Sun, L., He, B., Zhang, L., and Zhang, C.: Characteristics and trends of ambient ozone and nitrogen oxides at urban, suburban, and rural sites from 2011 to 2017 in Shenzhen, China, Sustainability-Basel, 10, 4530, https://doi.org/10.3390/su10124530, 2018.

Li, X., Zhang, F., Ren, J., Han, W., Zheng, B., Liu, J., Chen, L., and Jiang, S.: Rapid narrowing of the urban–suburban gap in air pollutant concentrations in Beijing from 2014 to 2019, Environmental Pollution, 304, 119146, https://doi.org/10.1016/j.envpol.2022.119146, 2022.

Tong, L., Zhang, H., Yu, J., He, M., Xu, N., Zhang, J., Qian, F., Feng, J., and Xiao, H.: Characteristics of surface ozone and nitrogen oxides at urban, suburban and rural sites in Ningbo, China, Atmos. Res., 187, 57-68, https://doi.org/10.1016/j.atmosres.2016.12.006, 2017.